*Clays and Clay Minerals*, Vol. 67, No. 6:537–544, 2019

# PHOTOREDUCTION OF METHYLVIOLOGEN IN SAPONITE CLAY: EFFECT OF METHYLVIOLOGEN ADSORPTION DENSITY ON THE REACTION EFFICIENCY

Takuya Fujimura[1]*, Tetsuya Shimada[2,3], Ryo Sasai[1], and Shinsuke Takagi[2,3]*

[1]Department of Materials Chemistry, Graduate School of Natural Science & Technology, Shimane University, 1060, Nishikawatsu-cho, Matsue, Shimane 690-8504, Japan

[2]Department of Applied Chemistry, Graduate School of Urban Environmental Sciences, Tokyo Metropolitan University, 1-1 Minami-osawa, Hachioji, Tokyo 192-0397, Japan

[3]Center for Artificial Photosynthesis, Tokyo Metropolitan University, 1-1 Minami-osawa, Hachioji, Tokyo 192-0397, Japan

**Abstract**—To identify the mechanisms for and to estimate the photochemical reaction efficiency of molecules in solid-state host materials is difficult. The objective of the present research was to measure the photogeneration efficiency of the methylviologen cation radical ($MV^{+}$•) hosted in a semi-transparent hybrid film composed of $MV^{2+}$ and saponite, a 2:1 clay mineral. $MV^{+}$• is the one-electron reduced species of $MV^{2+}$. $MV^{+}$• was generated by UV irradiation of these films. The fluorescence intensity of $MV^{2+}$ and the photogeneration efficiency of $MV^{+}$• depended on the loading level of $MV^{2+}$. When the loading level of $MV^{2+}$ was high (75% of the cation exchange capacity (abbreviated as % CEC) of saponite), its fluorescence was reduced considerably because of the self-fluorescence quenching reaction, and the photogeneration efficiency of $MV^{+}$• was relatively high (quantum yield $\varphi = 3.5\times10^{-2}$) compared to that of films with low adsorption density (10% CEC, $\varphi = 1.1\times10^{-2}$). Furthermore, when the loading level of $MV^{2+}$ was very low (0.13% CEC), a self-fluorescence quenching reaction was not observed and $MV^{+}$• was not generated. From these observations, one of the principal mechanisms of the self-quenching reaction and $MV^{+}$• formation in saponite is the electron transfer reaction between excited $MV^{2+}$ and adjacent $MV^{2+}$ molecules in the ground state.

**Keywords**—Methylviologen · Organic molecule–clay complex · Photoinduced electron transfer · Photoreduction · Self-fluorescence quenching hybrid film · Smectite

## INTRODUCTION

Over the last several decades, photoinduced hydrogen generation has been studied for the conversion of solar energy into chemical energy (Sprick et al. 2016; Stevenson et al. 2017; Wang et al. 2017). Methylviologen ($MV^{2+}$) has been used commonly to evolve hydrogen, because its one-electron reduced species (methylviologen cation radical, $MV^{+}$•) generates hydrogen in the presence of a Pt catalyst (Toshima et al. 1981; Matheson et al. 1983; Bard and Fox 2002). Many researchers have studied the generation of $MV^{+}$• and/or hydrogen from $MV^{2+}$ with visible light irradiation in the presence of photosensitizers (Wasielewski 1992; Yonemoto et al. 1992; Inoue et al. 1994). In addition, some researchers have found that, under UV light irradiation, $MV^{+}$• is generated in solution in the presence of solid surfaces such as silica gels, layered transition metal oxides, and zeolites (Miyata et al. 1988; Mao et al. 1995; Alvaro et al. 1997; Peon et al. 2001). Among inorganic layered materials, clay minerals are an attractive group because of their following properties: (1) flat surfaces; (2) regularly arranged anionic charges on their surfaces; (3) exfoliation and stackability of individual nanolayers depending on the medium; (4) optical transparency in the visible region in the exfoliated state when the particle size is small (<100 nm); and (5) easy formation of hybrid materials with cationic molecules by electrostatic interaction (Shichi & Takagi 2000; Egawa et al. 2011). Various researchers have reported hybrid materials of clay minerals and $MV^{2+}$ (Raupach et al. 1979; Villemure et al. 1986, 1991; Miyata et al. 1987; Rytwo et al. 1996), and Ogawa and co-workers (Kakegawa et al. 2003) reported that $MV^{+}$• was generated when intercalated $MV^{2+}$ in clay minerals was irradiated by UV light. The mechanism of $MV^{+}$• generation in clay minerals under UV light was mentioned as being due to the generation of $MV^{+}$• via an electron-transfer reaction from the bridging Si-O-Al oxygen lone pair to the excited $MV^{2+}$. However, in the solid hybrid systems above, estimating the efficiency of photogeneration of $MV^{+}$• was difficult, and the reaction details were not revealed because the amount of $MV^{+}$• generated and decreased amount of $MV^{2+}$ could not be estimated.

Previous work revealed the interesting structure of porphyrin–clay mineral hybrids, in which the porphyrin molecules adsorb densely on the exfoliated clay nanolayers without aggregation (Takagi et al. 2002, 2013). The crucial factor for the very dense adsorption of porphyrins was the matching of the distances between cationic sites in porphyrin and the average distance between anionic sites on the clay nanolayer surfaces (called the intercharge distance matching effect or size-matching effect). In these systems, the fluorescence intensity of some dyes adsorbed on saponite surfaces was quenched at higher adsorption densities (self-fluorescence quenching reaction) (Ishida et al. 2012b; Ohtani et al. 2014). This observation suggested that collision and/or electron transfer between excited and adjacent

* E-mail address of corresponding author:
tfujimura@riko.shimane-u.ac.jp
DOI: 10.1007/s42860-019-00047-8

**Electronic supplementary material** The online version of this article (https://doi.org/10.1007/s42860-019-00047-8) contains supplementary material, which is available to authorized users.

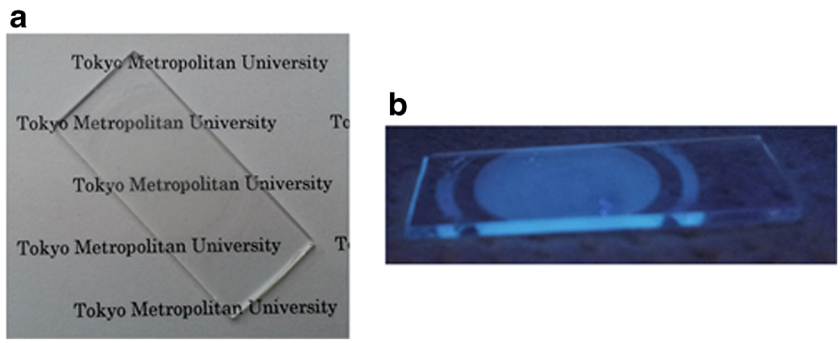


**Fig. 1.** Photographs of $MV^{2+}$/SSA hybrid film: (**a**) light transmission and (**b**) under UV irradiation

ground-state dye molecules might be one of the reasons for the self-fluorescence quenching reaction. The detail of the self-fluorescence quenching reaction, however, was not revealed.

$MV^{2+}$ adsorbed on clay minerals has been reported to show self-fluorescence quenching behavior (Villemure et al. 1986, 1991). Judging from those studies and previous results, the principal mechanism for the generation of $MV^{+}$• either on the surface or in the interlayer space of saponite could be an electron transfer reaction between the excited methylviologen (abbreviated as $MV^{2+}$*) and the adjacent ground-state $MV^{2+}$. The objective of the current study was to measure the photogeneration efficiency of $MV^{+}$• in a semi-transparent hybrid film composed of $MV^{2+}$ and saponite, in which the amount of $MV^{2+}$ and $MV^{+}$• could be estimated by UV-Vis absorption spectra, and to determine whether the principal mechanism of the self-fluorescence quenching reaction is indeed electron transfer between $MV^{2+}$* and the adjacent ground-state $MV^{2+}$ molecules, all with an eye to understanding whether this electron transfer reaction in the interlayer space of the clay mineral could be utilized further to construct other photochemical reaction systems.

## METHODS

### *Preparation of $MV^{2+}$/Saponite Hybrid Film*

A synthetic saponite (Sumecton SA ($(Na_{0.49}Mg_{0.14})[(Si_{7.20}Al_{0.80})(Mg_{5.97}Al_{0.03})O_{20}(OH)_4]$), abbreviated as SSA, from Kunimine Industries Co., Ltd., Chiyoda-ku, Tokyo, Japan) was used, and its theoretical surface area and CEC were 750 $m^2\ g^{-1}$ and 1.00 meq $g^{-1}$, respectively (Egawa et al. 2011). $MV^{2+}$ dichloride was purchased from Nacalai Tesque, Inc (>98%, Chukyo-ku, Kyoto, Japan). The purity of the $MV^{2+}$ was checked by $^1$H-NMR and thin layer chromatography. All of the chemicals were used as received.

Quartz substrates were sonicated with water for 30 min and then sonicated with ethanol for another 30 min. These substrates were further treated in sulfuric acid (Kanto Chemical, Chuo-ku, Tokyo, Japan) overnight at room temperature and washed with > 150 mL of water to remove the sulfuric acid. $MV^{2+}$/SSA hybrid films were prepared according to the literature (Kawamata et al. 2010; Takagi et al. 2004, 2010; Suzuki et al. 2011). $MV^{2+}$ aqueous solution ($2.0\times10^{-4}$ mol/L, 600 μL) was added to the saponite dispersion (2400 μL) within 2 s to prepare a $MV^{2+}$/SSA complex dispersion in the exfoliated state (Suquet et al. 1977; Auerbach et al. 2004). The $MV^{2+}$ loading level as a fraction of the % CEC of the clay mineral was adjusted from 10 to 80% CEC by changing the concentration of the saponite dispersion (from 1.00 to $1.25\times10^{-1}$ g/L). The complex dispersions were filtered through PTFE membrane filters (pore size = 0.1 μm, Advantec, Bunkyo-ku, Tokyo, Japan). The residue was transferred onto a quartz substrate (Agri, Oume-city, Tokyo, Japan) and dried under vacuum overnight at room temperature to form a semi-transparent $MV^{2+}$/SSA hybrid film.

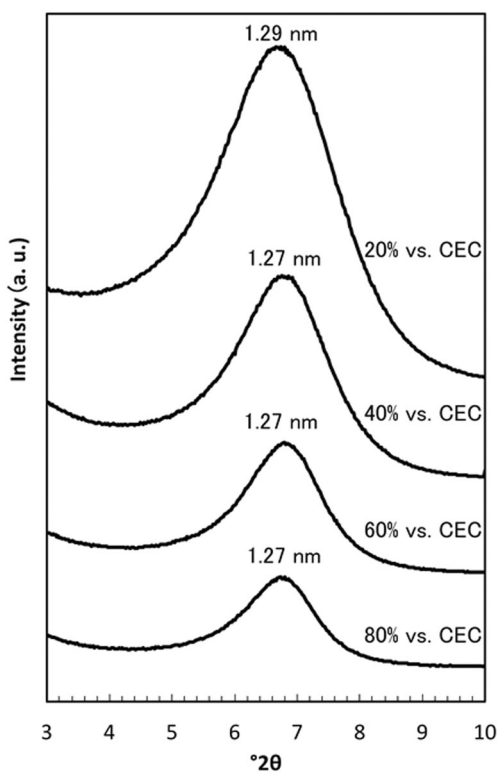


**Fig. 2.** XRD patterns of $MV^{2+}$/SSA hybrid films, with $MV^{2+}$ loading levels of 20%, 40%, 60%, and 80% CEC

https://doi.org/10.1007/s42860-019-00047-8 Published online by Cambridge University Press

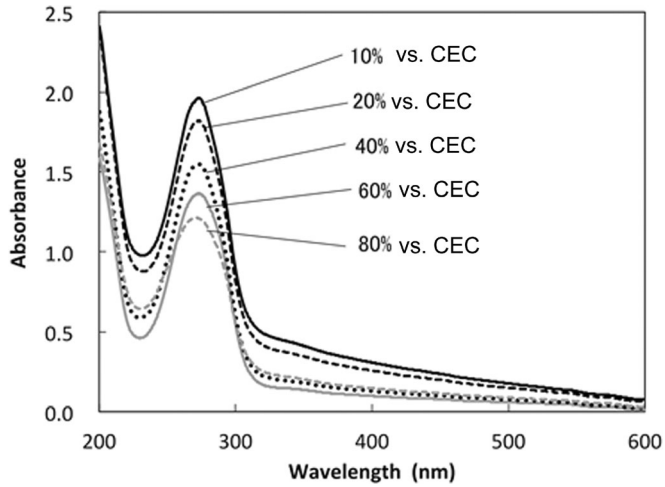


**Fig. 3.** UV-Vis absorption spectra of $MV^{2+}$/SSA hybrid films, with $MV^{2+}$ loading levels of 10% (black solid line), 20% (black broken line), 40% (black dotted line), 60% (gray solid line), and 80% (gray broken line) CEC

*Photogeneration of $MV^{+}$• in Hybrid Film*

$MV^{2+}$/hybrid films were placed in a cuvette and vacuumed for >1 h to remove the oxygen that quenches $MV^{+}$•. These films were irradiated with UV light (270 nm, FWHM of wavelength was 12 nm) from a Xe lamp through a diffraction grating to examine the photoreduction of $MV^{2+}$. The generation of $MV^{+}$• was monitored with a UV-Vis absorption spectrometer. The cuvette was kept under vacuum during photo-irradiation and measurement of UV-Vis absorption spectra.

*Analysis*

The UV-Vis absorption spectra were obtained on a UV-3150 system (Shimadzu, Chukyo-ku, Kyoto, Japan). The fluorescence spectra were measured using an FP-6600 spectrofluorometer (Jasco, Hachioji-city, Tokyo, Japan), with an excitation wavelength of 272 nm. The hybrid film was set at 45° relative to the axis of the excitation beam and the emission detector. X-ray diffraction (XRD) patterns were measured using a RINT TTR III system (Rigaku, Akishima-city, Tokyo, Japan), using CuKα radiation. These measurements were carried out at room temperature.

## RESULTS AND DISCUSSION

*XRD Patterns and Absorption and Fluorescence Spectra of the Hybrid Film*

The hybrid film was sufficiently transparent (Fig. 1a) for transmission-mode measurements. The photograph of the hybrid film under 254 nm UV light irradiation (Fig. 1b) revealed blue or purple emission from $MV^{2+}$*, while $MV^{2+}$ in the aqueous medium exhibited no emission. Fluorescence was observed, however, when $MV^{2+}$ was intercalated in the clay

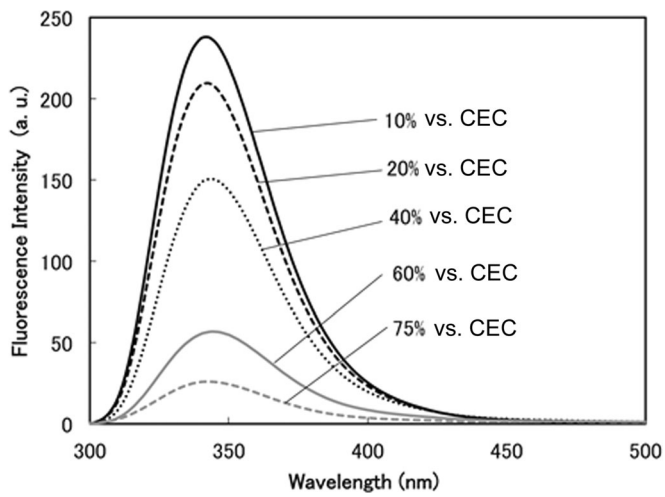


**Fig. 4.** Fluorescence spectra of $MV^{2+}$/SSA hybrid films at various $MV^{2+}$ loadings, with $MV^{2+}$ loading levels of 10% (black solid line), 20% (black broken line), 40% (black dotted line), 60% (gray solid line), and 80% (gray broken line) CEC. The excitation wavelength was set at 272 nm

https://doi.org/10.1007/s42860-019-00047-8 Published online by Cambridge University Press

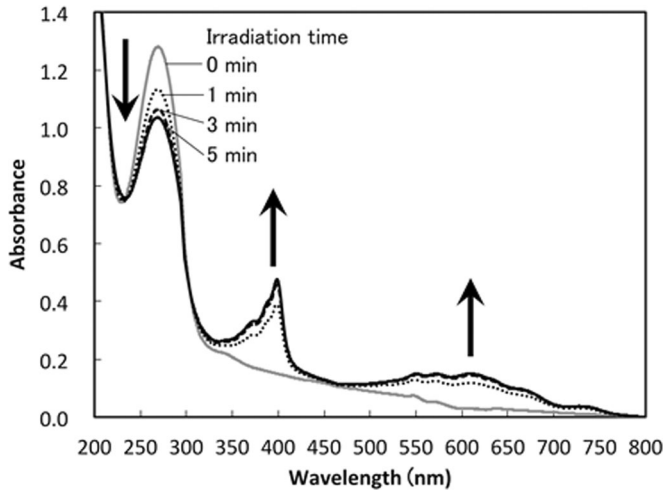


**Fig. 5.** UV-Vis absorption spectra of $MV^{2+}$/SSA hybrid film during UV-irradiation (concentration of $MV^{2+}$: 75% CEC) at 0 min (gray solid line), 1 min (black dotted line), 3 min (black broken line), and 5 min (black solid line)

mineral or adsorbed on the clay surfaces, as reported by Detellier and Szabo (Villemure et al. 1986, 1991). The rotation of pyridyl groups of $MV^{2+}$ was suppressed by adsorption on the SSA surface, and then the rate constant of non-radiative deactivation decreased. This phenomenon has been commonly recognized as surface-fixation induced emission (S-FIE) (Ishida et al. 2014; Tokieda et al. 2017).

From the XRD patterns of $MV^{2+}$/SSA hybrid films at various $MV^{2+}$ loading levels (Fig. 2), the interlayer spaces of hybrid films were estimated to be 0.30–0.32 nm, which is almost the same as that of montmorillonite and other clay minerals where $MV^{2+}$ was intercalated (Raupach et al. 1979; Rytwo et al. 1996; Kakegawa et al. 2003). Judging from the thickness of pyridyl groups and the basal space of SSA in the hybrid film, the orientation of $MV^{2+}$ aromatic rings in the interlayer of SSA was parallel to the SSA layer. The XRD pattern of $MV^{2+}$/SSA shifted slightly to a higher diffraction angle, indicating the decrease in interlayer distance, when the loading level of $MV^{2+}$ was increased. This may indicate that the interlayer space of $MV^{2+}$/SSA hybrid film became hydrophobic with the increased $MV^{2+}$, and then the interlayer water was excluded.

The UV-Vis absorption spectra of hybrid films varied with different loading levels of $MV^{2+}$ (Fig. 3). The film with no $MV^{2+}$ loading displayed no absorption band in the 200–600 nm region (not shown). The background of each film was different because of the scattering by SSA; however, the absorption band ascribed to $MV^{2+}$ was clearly observed in the UV region in all cases. Note that when the loading level of $MV^{2+}$ was low, a correspondingly greater amount of SSA was in the film, thus causing greater scattering. The maximum absorption wavelength ($\lambda_{max}$) of $MV^{2+}$ was shifted to longer wavelength (272 nm) compared to that in the aqueous solution (257 nm, Fig. S1). A similar spectral shift was observed when $MV^{2+}$ was adsorbed on the surfaces of SSA or other clay minerals (Villemure et al. 1991). This result indicated that the π-conjugated system of $MV^{2+}$ was extended by the co-planarization of its two pyridinium groups (Fig. S2) because of the steric effect of SSA (Kuykendall & Thomas 1990; Chernia & Gill 1999; Ishida et al. 2012a). The $\lambda_{max}$ of $MV^{2+}$ was independent of the $MV^{2+}$ loading level, and the spectral shape was also almost the same. Hence, the $MV^{2+}$ intercalated in the interlayer of SSA did not aggregate in spite of its dense intercalation. When the $MV^{2+}$ loading level in the hybrid film

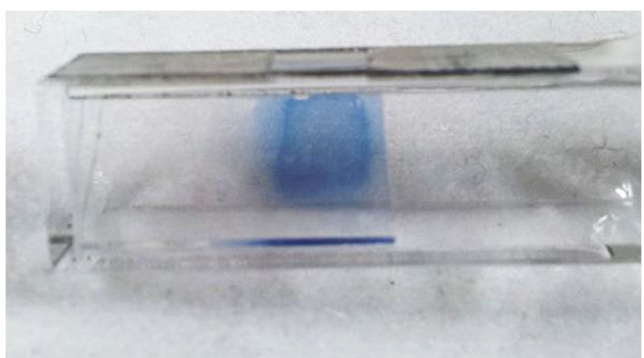

**Fig. 6.** Photograph of $MV^{2+}$/SSA hybrid film after UV light irradiation

https://doi.org/10.1007/s42860-019-00047-8 Published online by Cambridge University Press

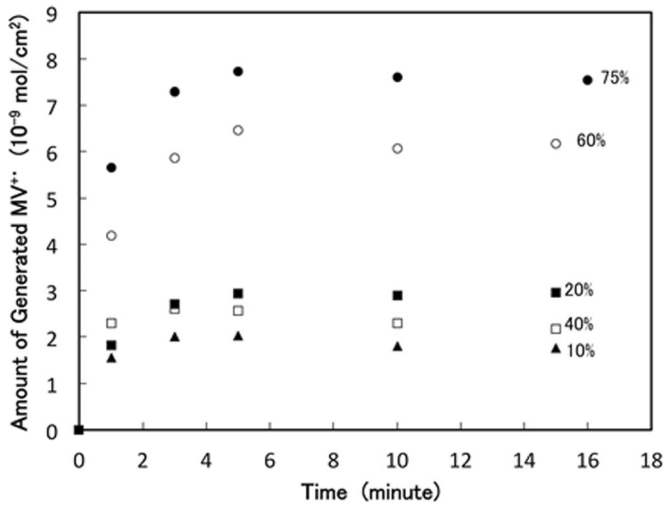


**Fig. 7.** Generation of $MV^{+}$• with UV irradiation at different $MV^{2+}$ loading levels: 75% (open circle), 60% (solid circle), 40% (open square), 20% (solid square), and 10% (solid triangle) CEC

was set as high as 80% CEC, the absorbance at 272 nm was relatively small compared to other films, and $MV^{2+}$ was observed in the filtrate, according to the UV-Vis absorption spectra. This indicated that a small amount of $MV^{2+}$ was not adsorbed on SSA, because its saturation adsorption amount on the SSA surface was <80% CEC. Judging from the optical absorbance of excess $MV^{2+}$ in the filtrate solution and the extinction coefficient of $MV^{2+}$ at 257 nm ($\varepsilon$ = 20700 mol·$L^{-1}$·$cm^{-1}$), the maximum adsorption of $MV^{2+}$ in the above hybrid film was calculated more accurately to be 75% CEC (Watanabe & Honda 1982). In the fluorescence spectra of $MV^{2+}$/SSA hybrid films (Fig. 4), fluorescence of $MV^{2+}$ was observed at the maximum emission wavelength of 344 nm.

The fluorescence of $MV^{2+}$ is known to occur when $MV^{2+}$ is adsorbed on/intercalated in clay minerals, although aqueous solutions of $MV^{2+}$ do not show the fluorescence (Villemure et al. 1986, 1991). This phenomenon is explained as being due to the suppression of rotation of the pyridinium groups of $MV^{2+}$ by the steric effect of the clay minerals, and the rate constant of internal conversion is decreased, as described above.

The shape of the emission spectrum was independent of the loading level of $MV^{2+}$. This suggests the absence of new luminescent species, such as J-type aggregates (head-to-tail type aggregate), and of excimers that could be formed in the interlayer space of SSA nanolayers, in spite of the large $MV^{2+}$ loadings. The emission intensities of $MV^{2+}$/SSA hybrid films decreased when the loading level of $MV^{2+}$ was increased, in spite of the same amount of $MV^{2+}$. The formation of H-type aggregates, which is one cause of fluorescence quenching, was not observed judging from the above-mentioned XRD and absorption spectra analyses. These results indicate that the fluorescence of $MV^{2+}$ was quenched via a self-fluorescence quenching reaction. The occupied surface area of an anion on SSA was calculated as 1.25 $nm^2$, based on the theoretical surface area and the cation exchange capacity. On the other hand, assuming that $MV^{2+}$ is rectangular (dihedral angle of pyridinium substrate is 0°), the cross-sectional footprint of $MV^{2+}$ would be 0.844 $nm^2$/molecule (viewed from the normal direction of the pyridinium group (Raupach et al. 1979). Calculating from these values, the occupancy ratio of the SSA surface by $MV^{2+}$ was 50% (at 75% CEC). Judging from the result of this calculation, $MV^{2+}$ should be intercalated into SSA without aggregation.

### *Generation of $MV^{+}$• with UV Irradiation in the Interlayer of Saponite*

The UV-Vis absorption spectra of $MV^{2+}$/SSA hybrid films (75% CEC) changed under UV irradiation at 270 nm (Fig. 5); the absorbance of $MV^{2+}$ decreased quickly under UV irradiation, and new absorption bands appeared at ~400 and ~600 nm. The newly appeared absorption bands at ~350–420 nm, the broadened band at ~450–750 nm, and their characteristic vibrational structures were almost the same as in the reported absorption spectrum of $MV^{+}$•, which is the one-electron reduced species of $MV^{2+}$ (Watanabe & Honda 1982; Bockman & Kochi 1990). In the photograph of the $MV^{2+}$/SSA hybrid film after UV irradiation (Fig. 6), the color of the film changed from colorless to blue, the latter being the typical color of $MV^{+}$• (Palenzuela et al. 2014). In addition, this absorption peak disappeared upon exposure to air, and then the absorption band of $MV^{2+}$ increased. This result also supports the conclusion that the newly generated species was $MV^{+}$• because it reacted with oxygen in air to produce $MV^{2+}$. The peak absorption wavelengths of $MV^{+}$• in the interlayer space of SSA were 398 and 608 nm. Interestingly, $\lambda_{max}$ of $MV^{+}$• was shifted slightly to a longer wavelength (by 2 nm) compared to that in water, although the $\lambda_{max}$ of $MV^{2+}$ was shifted to an even longer wavelength (by >10 nm) by intercalation into the interlayer space of SSA. These observations could be ascribed to the different stable structures of $MV^{2+}$ and $MV^{+}$• in water. In the case of $MV^{2+}$, the pyridinium groups are not co-planar in water because of the steric effect, while the stable structure of $MV^{+}$• is approximately co-planar (Bockman & Kochi 1990; Kubota 1999; Porter & Vaid 2005). Thus, the $\lambda_{max}$

https://doi.org/10.1007/s42860-019-00047-8 Published online by Cambridge University Press

**Table 1.** Quantum yields (φ) of the $MV^{+}$• photogeneration in hybrid films

| Loading level of $MV^{2+}$ (% CEC) | 10 | 20 | 40 | 60 | 75 |
|---|---|---|---|---|---|
| φ (%) | 1.1 | 0.9 | 1.1 | 2.4 | 3.5 |

of intercalated $MV^{+}$• in SSA was almost the same as in water, because the effect of co-planarization by intercalation is relatively weak compared to that for $MV^{2+}$. $MV^{+}$• was not generated without UV light irradiation, indicating that the $MV^{2+}$ intercalated in SSA was reduced by UV irradiation.

Several reports have discussed the photoreduction of $MV^{2+}$ with UV irradiation in several media, such as water, organic solvents, and solid surfaces, as mentioned above. The electron donor to reduce the $MV^{2+}$ via a photoinduced electron transfer reaction was discussed in those reports. Although some reports indicated that the chloride ion is the electron donor to reduce $MV^{2+}$* (Ebbesen et al. 1984; Peon et al. 2001), $MV^{2+}$ adsorbs on SSA by electrostatic interaction and, thus, few chloride ions should be present in the hybrid film. Kohler and co-workers (Peon et al. 2001) reported that gas-phase water has a high ionization potential (12.62 eV), and they did not observe the quenching of $MV^{2+}$* via electron transfer. Considering the previous reports, the residual interlayer water should not be the electron donor. In aluminosilicate media (clays and zeolites), some reports (Alvaro et al. 1997; Kakegawa et al. 2003) suggested that the bridging Si-O-Al oxygen lone pair can donate an electron to $MV^{2+}$*. To confirm this electron transfer pathway, $MV^{2+}$/SSA hybrid films with very low adsorption density of $MV^{2+}$ (0.13% and 0.06% CEC) were prepared to avoid the self-fluorescence quenching reaction. The fluorescence intensities of these films were approximately the same in spite of their different loading levels of $MV^{2+}$. Thus, the self-quenching reaction was absent in these films (Fig. S3). The UV-Vis absorption spectra of $MV^{2+}$/SSA hybrid film ($MV^{2+}$ loading level of 0.13% CEC) varied during UV irradiation (Fig. S4). The absorbance ascribed to $MV^{2+}$ decreased with UV irradiation because of decomposition after prolonged UV exposure, and a small absorption band was observed at ~400 nm. The absorption peak at ~600 nm attributed to $MV^{+}$•, however, was not observed, and the existing peak did not disappear in the presence of oxygen. These observations suggested that $MV^{+}$• was not generated because it would be quenched by oxygen molecules. This absorption band was similar to that of the decomposition product of $MV^{2+}$ (Solar et al. 1982; Bahnemann et al. 1987). Hence, the new species was not $MV^{+}$• but a decomposition product. All these results, taken together, indicate that the electron transfer from the bridging Si-O-Al oxygen lone pair to $MV^{2+}$* did not take place. Considering these results and the dependency of $MV^{+}$• photogeneration on the adsorption density of $MV^{2+}$ (as described below), the photoinduced electron transfer reaction between excited $MV^{2+}$ and adjacent ground-state $MV^{2+}$ would be one of the principal pathways of the self-quenching reaction. An electron transfer reaction between electron donor and acceptor depends on their redox potentials and re-organization energy, requiring a difference between the reduction potential of the acceptor and the oxidation potential of the donor. In this case, the redox potential of $MV^{2+}$ would be affected by the negative charges of SSA and co-planarization of the dye molecules, both of which will depend on the distance between the anionic site on SSA and the cationic site of $MV^{2+}$. Thus, a difference in the adsorption site might change the redox potentials slightly, thereby allowing the photoinduced electron transfer reaction to happen.

Although a back electron transfer reaction between $MV^{+}$• and oxidized $MV^{2+}$ was expected, $MV^{+}$• could be observed by the typical steady-state UV-Vis spectrophotometer. The reason is that the one-electron oxidized $MV^{2+}$ will be unstable and, thus, undergo a decomposition reaction, and then the back electron transfer may be suppressed.

The generation of $MV^{+}$• with UV irradiation in $MV^{2+}$/SSA hybrid films at various adsorption densities of $MV^{2+}$ is summarized in Fig. 7. The amount of $MV^{+}$• generated was calculated from $\Delta abs. = abs_t - abs_0$ and the extinction coefficient of $MV^{+}$• in water (Watanabe & Honda 1982). The amount of $MV^{+}$• generated depended on the adsorption density of $MV^{2+}$, and reached a plateau in all hybrid films. The maximum conversion ratio from $MV^{2+}$ to $MV^{+}$• (generated $MV^{+}$• / initial $MV^{2+}$) was 0.144 (75% CEC), although the maximum value of the conversion ratio will be 0.5. This is because $MV^{2+}$* may be quenched by the $MV^{+}$• generated and decomposition products. According to the quantum yield (φ) at 1 min of the photogeneration of $MV^{+}$• (Table 1), the photogeneration efficiency of $MV^{+}$• increased with increasing adsorption density of $MV^{2+}$, indicating that the self-fluorescence quenching reaction is important for generating $MV^{+}$•. φ drastically increased at large dye loadings (>60% CEC), suggesting that the roaming range of $MV^{2+}$* within the excited lifetime will be limited, because $MV^{2+}$ molecules have to approach each other to some extent.

## CONCLUSIONS

The generation of $MV^{+}$• in semi-transparent $MV^{2+}$/SSA hybrid films under UV irradiation was observed clearly by transmission spectra. The efficiency of $MV^{+}$• generation depended on the adsorption density of $MV^{2+}$. When the adsorption density of $MV^{2+}$ was low, where a self-quenching reaction was not observed, $MV^{+}$• was not generated. This indicates that $MV^{+}$• was produced via electron transfer between $MV^{2+}$* and $MV^{2+}$ on the saponite surfaces.

## ACKNOWLEDGMENTS

This work was partly supported by the PRESTO/JST Program, Innovative Use of Light and Materials/Life; a Grant-in-Aid for Scientific Research on Innovative Areas; a Grant-in-Aid for Scientific Research (B) (No. 24350100); and a Grant-in-Aid for Scientific Research on Innovative Areas "All Nippon Artificial Photosynthesis Project for Living Earth" (AnApple, No. 25107521).

https://doi.org/10.1007/s42860-019-00047-8 Published online by Cambridge University Press

## REFERENCES


Alvaro, M., García, H., García, S., Márquez, F., & Scaiano, J. C. (1997). Intrazeolite photochemistry. 17. Zeolites as electron donors: Photolysis of methylviologen incorporated within zeolites. *The Journal of Physical Chemistry B, 101*, 3043–3051.

Auerbach, S. M., Carrado, K. A., & Dutta, P. K. (2004). *Handbook of Layered Materials, 10*. Florida: CRC Press.

Bahnemann, D. W., Fischer, C.-H., Janata, E., & Henglein, A. (1987). The two-electron oxidation of methyl viologen. Detection and analysis of two fluorescing products. *Journal of the Chemical Society, Faraday Transactions 1: Physical Chemistry in Condensed Phases, 83*, 2559.

Bard, A. J., & Fox, M. A. (2002). Artificial photosynthesis: Solar splitting of water to hydrogen and oxygen. *Accounts of Chemical Research, 28*, 141–145.

Bockman, T. M., & Kochi, J. K. (1990). Isolation and oxidation-reduction of methylviologen cation radicals. Novel disproportionation in charge-transfer salts by X-ray crystallography. *The Journal of Organic Chemistry, 55*, 4127–4135.

Chernia, Z., & Gill, D. (1999). Flattening of tmpyp adsorbed on laponite. Evidence in observed and calculated UV−vis spectra. *Langmuir, 15*, 1625–1633.

Ebbesen, T. W., Manring, L. E., & Peters, K. S. (1984). Picosecond photochemistry of methyl viologen. *Journal of the American Chemical Society, 106*, 7400–7404.

Egawa, T., Watanabe, H., Fujimura, T., Ishida, Y., Yamato, M., Masui, D., Shimada, T., Tachibana, H., Yoshida, H., Inoue, H., & Takagi, S. (2011). Novel methodology to control the adsorption structure of cationic porphyrins on the clay surface using the "size-matching rule". *Langmuir, 27*, 10722–10729.

Inoue, H., Ichiroku, N., Torimoto, T., Sakata, T., Mori, H., & Yoneyama, H. (1994). Photoinduced electron transfer from zinc sulfide microcrystals modified with various alkanethiols to methyl viologen. *Langmuir, 10*, 4517–4522.

Ishida, Y., Masui, D., Shimada, T., Tachibana, H., Inoue, H., & Takagi, S. (2012a). The mechanism of the porphyrin spectral shift on inorganic nanosheets: The molecular flattening induced by the strong host–guest interaction due to the "size-matching rule". *The Journal of Physical Chemistry C, 116*, 7879–7885.

Ishida, Y., Shimada, T., Tachibana, H., Inoue, H., & Takagi, S. (2012b). Regulation of the collisional self-quenching of fluorescence in clay/porphyrin complex by strong host-guest interaction. *The Journal of Physical Chemistry A, 116*, 12065–12072.

Ishida, Y., Shimada, T., & Takagi, S. (2014). "Surface-fixation induced emission" of porphyrazine dye by a complexation with inorganic nanosheets. *The Journal of Physical Chemistry C, 118*, 20466–20471.

Kakegawa, N., Kondo, T., & Ogawa, M. (2003). Variation of electron-donating ability of smectites as probed by photoreduction of methyl viologen. *Langmuir, 19*, 3578–3582.

Kawamata, J., Suzuki, Y., & Tenma, Y. (2010). Fabrication of clay mineral–dye composites as nonlinear optical materials. *Philosophical Magazine, 90*, 2519–2527.

Kodaka, M., & Kubota, Y. (1999). Effect of structures of bipyridinium salts on redox potential and its application to $CO_2$ fixation. *Journal of the Chemical Society, Perkin Transactions, 2*, 891–894.

Kuykendall, V. G., & Thomas, J. K. (1990). Photophysical investigation of the degree of dispersion of aqueous colloidal clay. *Langmuir, 6*, 1350–1356.

Mao, Y., Breen, N. E., & Thomas, J. K. (1995). Formation of methylviologen radical monopositive cations and ensuing reactions with polychloroalkanes on silica gel surfaces. *The Journal of Physical Chemistry, 99*, 9909–9917.

Matheson, M. S., Lee, P. C., Meisel, D., & Pelizzetti, E. (1983). Kinetics of hydrogen production from methyl viologen radicals on colloidal platinum. *The Journal of Physical Chemistry, 87*, 394–399.

Miyata, H., Sugahara, Y., Kuroda, K., & Kato, C. (1987). Synthesis of montmorillonite–viologen intercalation compounds and their photochromic behaviour. *Journal of the Chemical Society, Faraday Transactions 1: Physical Chemistry in Condensed Phases, 83*, 1851.

Miyata, H., Sugahara, Y., Kuroda, K., & Kato, C. (1988). Synthesis of a viologen–tetratitanate intercalation compound and its photochemical behaviour. *Journal of the Chemical Society, Faraday Transactions 1: Physical Chemistry in Condensed Phases, 84*, 2677.

Ohtani, Y., Ishida, Y., Ando, Y., Tachibana, H., Shimada, T., & Takagi, S. (2014). Adsorption and photochemical behaviors of the novel cationic xanthene derivative on the clay surface. *Tetrahedron Letters, 55*, 1024–1027.

Palenzuela, J., Vinuales, A., Odriozola, I., Cabanero, G., Grande, H. J., & Ruiz, V. (2014). Flexible viologen electrochromic devices with low operational voltages using reduced graphene oxide electrodes. *ACS Applied Materials & Interfaces, 6*, 14562–14567.

Peon, J., Tan, X., Hoerner, J. D., Xia, C., Luk, Y. F., & Kohler, B. (2001). Excited state dynamics of methyl viologen. Ultrafast photoreduction in methanol and fluorescence in acetonitrile. *The Journal of Physical Chemistry A, 105*, 5768–5777.

Porter 3rd, W. W., & Vaid, T. P. (2005). Isolation and characterization of phenyl viologen as a radical cation and neutral molecule. *The Journal of Organic Chemistry, 70*, 5028–5035.

Raupach, M., Emerson, W. W., & Slade, P. G. (1979). The arrangement of paraquat bound by vermiculite and montmorillonite. *Journal of Colloid and Interface Science, 69*, 398–408.

Rytwo, G., Nir, S., & Margulies, L. (1996). Adsorption and interactions of diquat and paraquat with montmorillonite. *Soil Science Society of America Journal, 60*, 601.

Shichi, T., & Takagi, K. (2000). Clay minerals as photochemical reaction fields. *Journal of Photochemistry and Photobiology C: Photochemistry Reviews, 1*, 113–130.

Solar, S., Solar, W., Getoff, N., Holcman, J., & Sehested, K. (1982). Pulse radiolysis of methyl viologen in aqueous solutions. *Journal of the Chemical Society, Faraday Transactions 1: Physical Chemistry in Condensed Phases, 78*, 2467.

Sprick, R. S., Bonillo, B., Clowes, R., Guiglion, P., Brownbill, N. J., Slater, B. J., Blanc, F., Zwijnenburg, M. A., Adams, D. J., & Cooper, A. I. (2016). Visible-light-driven hydrogen evolution using planarized conjugated polymer photocatalysts. *Angewandte Chemie International Edition, 55*, 1792–1796.

Stevenson, M. J., Marguet, S. C., Schneider, C. R., & Shafaat, H. S. (2017). Light-driven hydrogen evolution by nickel-substituted rubredoxin. *ChemSusChem, 10*, 1–7.

Suquet, H., Iiyama, J. T., Kodama, H., & Pezerat, H. (1977). Synthesis and swelling properties of saponites with increasing layer charge. *Clays and Clay Minerals, 25*, 231–242.

Suzuki, Y., Tenma, Y., Nishioka, Y., Kamada, K., Ohta, K., & Kawamata, J. (2011). Efficient two-photon absorption materials consisting of cationic dyes and clay minerals. *The Journal of Physical Chemistry C, 115*, 20653–20661.

Takagi, S., Tryk, D. A., & Inoue, H. (2002). Photochemical energy transfer of cationic porphyrin complexes on clay surface. *Journal of Physical Chemistry B, 106*, 5455–5460.

Takagi, S., Eguchi, M., Yui, T., & Inoue, H. (2004). Photochemical electron transfer reactions in clay-porphyrin complexes. *Clay Science, 12*, 82–87.

Takagi, S., Shimada, T., Masui, D., Tachibana, H., Ishida, Y., Tryk, D. A., & Inoue, H. (2010). Unique solvatochromism of a membrane composed of a cationic porphyrin-clay complex. *Langmuir, 26*, 4639–4641.

Takagi, S., Shimada, T., Ishida, Y., Fujimura, T., Masui, D., Tachibana, H., Eguchi, M., & Inoue, H. (2013). Size-matching effect on inorganic nanosheets: Control of distance, alignment, and orientation of molecular adsorption as a bottom-up methodology for nanomaterials. *Langmuir, 29*, 2108–2119.

Tokieda, D., Tsukamoto, T., Ishida, Y., Ichihara, H., Shimada, T., & Takagi, S. (2017). Unique fluorescence behavior of dyes on the clay minerals surface: Surface fixation induced emission (s-fie). *Journal of Photochemistry and Photobiology A: Chemistry, 339*, 67–79.

Toshima, N., Kuriyama, M., Yamada, Y., & Hirai, H. (1981). Colloidal platinum catalyst for light-induced hydrogen evolution from water. A particle size effect. *Chemistry Letters, 10*, 793–796.

Villemure, G., Detellier, C., & Szabo, A. G. (1986). Fluorescence of clay-intercalated methylviologen. *Journal of the American Chemical Society, 108*, 4658–4659.

Villemure, G., Detellier, C., & Szabo, A. G. (1991). Fluorescence of methylviologen intercalated into montmorillonite and hectorite aqueous suspensions. *Langmuir, 7*, 1215–1221.

Wang, Q., Hisatomi, T., Suzuki, Y., Pan, Z., Seo, J., Katayama, M., Minegishi, T., Nishiyama, H., Takata, T., Seki, K., Kudo, A., Yamada, T., & Domen, K. (2017). Particulate photocatalyst sheets based on carbon conductor layer for efficient z-scheme pure-water splitting at ambient pressure. *Journal of the American Chemical Society, 139*, 1675–1683.

Wasielewski, M. R. (1992). Photoinduced electron transfer in supramolecular systems for artificial photosynthesis. *Chemical Reviews, 92*, 435–461.

Watanabe, T., & Honda, K. (1982). Measurement of the extinction coefficient of the methyl viologen cation radical and the efficiency of its formation by semiconductor photocatalysis. *The Journal of Physical Chemistry, 86*, 2617–2619.

Yonemoto, E. H., Riley, R. L., Kim, Y. I., Atherton, S. J., Schmehl, R. H., & Mallouk, T. E. (1992). Photoinduced electron transfer in covalently linked ruthenium tris(bipyridyl)-viologen molecules: Observation of back electron transfer in the Marcus inverted region. *Journal of the American Chemical Society, 114*, 8081–8087.

(*Received 15 September 2018; revised 11 December 2019; AE: J. Brendlé-Miehé*)

https://doi.org/10.1007/s42860-019-00047-8 Published online by Cambridge University Press